

Surface Display of a Redox Enzyme and its Site-Specific Wiring to Gold Electrodes

Liron Amir,^{†,‡,§,||} Stewart A. Carnally,^{†,‡,||} Josep Rayo,^{§,||} Shaked Rosenne,^{§,||} Sarit Melamed Yerushalmi,^{§,||} Orr Schlesinger,^{†,‡,||} Michael M. Meijler,^{*,§,||} and Lital Alfonta^{*,†,‡,||}

[†]The Avram and Stella Goldstein-Goren Department of Biotechnology Engineering, [‡]Ilse Katz Institute for Nanoscale Science and Technology, [§]Department of Chemistry, and ^{||}National Institute for Biotechnology in the Negev, P.O. Box 653, Ben-Gurion University of the Negev, Beer-Sheva 84105, Israel

S Supporting Information

ABSTRACT: The generation of a current through interaction between bacteria and electrodes has been explored by various methods. We demonstrate the attachment of living bacteria through a surface displayed redox enzyme, alcohol dehydrogenase II. The unnatural amino acid para-azido-L-phenylalanine was incorporated into a specific site of the displayed enzyme, facilitating electron transfer between the enzyme and an electrode. In order to attach the bacteria carrying the surface displayed enzyme to a surface, a linker containing an alkyne and a thiol moiety on opposite ends was synthesized and attached to the dehydrogenase site specifically through a copper(I)-catalyzed azide–alkyne cycloaddition reaction. Using this approach we were able to covalently link bacteria to gold-coated surfaces and to gold nanoparticles, while maintaining viability and catalytic activity. We show the performance of a biofuel cell using these modified bacteria at the anode, which resulted in site-specific dependent fuel cell performance for at least a week. This is the first example of site-specific attachment of a true living biohybrid to inorganic material.

The attachment of biomolecules and whole organisms to surfaces has been studied for several decades for a plethora of applications. Enzymes, antibodies, and antigens were immobilized for a wide range of uses, such as biosensing,^{1–4} logic gates,⁵ biofuel cells,^{6,7} bioelectronics,⁸ proteomics,⁹ and diagnostics.^{10–13} Cells and microorganisms were previously attached to surfaces by various approaches.^{14,15} Different chemistries were used for the attachment of amino acid residues of the biomolecules to surfaces. One of the drawbacks of these applied chemical approaches is that they are not specific and often target functional groups at undesired locations on the surface of a given protein, compromising activity. Our approach is general and could be adapted to any redox enzyme or any protein for that matter (including antibodies), provides the enzyme with the right orientation relative to the surface, and includes a single population of enzymes relative to the electrode. Hence, it is much more accurate in data interpretation. Here, we report the first example of site specifically oriented surface displayed enzymes through which entire microorganisms are covalently attached to gold electrodes or nanoparticles. Notably, the immobilized

microorganisms maintain viability, while the displayed redox enzymes are active and the sites of modification determine their specific activity.

We set out to prepare such a system, as described in Figure 1A: *Escherichia coli* JK321 strain (*E. coli*) was used for the

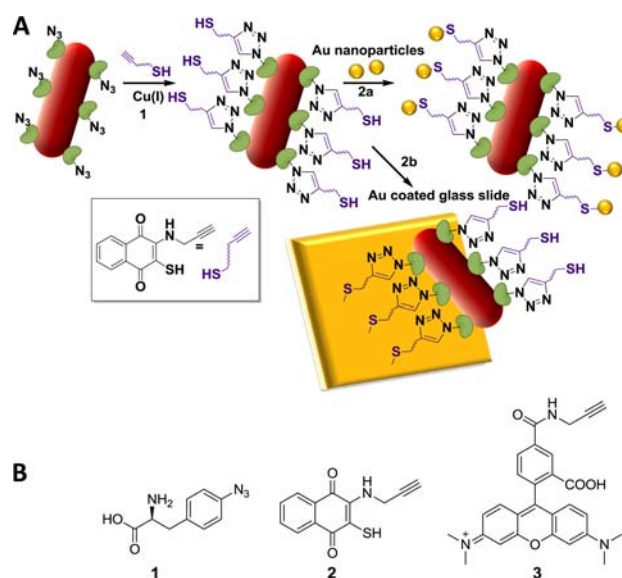


Figure 1. (A) (1) Scheme for the specific cycloaddition of the linker to azide-bearing unnatural amino acid (UAA) on surface displayed ADH II. (2a) Attachment of gold nanoparticles via thiol linkage; (2b) attachment of whole cells to gold surface. (B) (1) *p*-azidophenylalanine (Az-Phe); (2) redox-active linker, containing alkyne and thiol moieties; (3) rhodamine-alkyne.

autodisplay¹⁶ of the enzyme alcohol dehydrogenase II (ADHII) from *Zymomonas mobilis* (*Z. mobilis*). In addition, the unnatural amino acid (UAA) *para*-azido-L-phenylalanine (Az-Phe)¹⁷ (1, Figure 1B) was incorporated into the surface displayed ADHII into specific sites (V66, P182, D314) in response to the stop codon TAG and resulted in the mutant enzymes V66TAG, P182TAG, D314TAG, respectively. Mutation locations were determined from a model of the crystal structure of a monomer of ADHII (Figure S1). Upon Az-Phe incorporation, we used a

Received: October 26, 2012

Published: December 11, 2012

specific redox linker (**2**, Figure 1B) that could be reacted from one side with the azide functional group on the enzyme (via copper(I) mediated alkyne–azide “click” cycloaddition) reaction¹⁸ and with a gold surface or a gold nanoparticle from its free side via a thiol group.

We reasoned that this approach could be advantageous in the design of efficient biosensors or biofuel cells based on living cells. Among the many advantages of a surface display system which permits presentation of an active enzyme on the surface of a microorganism are: the elimination of the need for enzyme purification,¹⁹ enhanced enzyme stability due to its proximity to the membrane,²⁰ and allowing for genetically encoded regeneration of the same enzyme once it loses activity,^{21,22} specifically when covalently attached to an inorganic surface. These three major advantages have been the incentive for our experimental design. In addition, the attachment of the surface displayed enzymes to gold through a redox active molecule allows us to direct the electrons that are released from fuel oxidation directly through the linker to the electrode. When used in biofuel cells, this allows the use of such a modified electrode as an anode that is not separated by a membrane from the cathode, since oxygen is not able to compete with the electrode over electrons.²³ Thus, all electrons directly released from fuel oxidation flow to the electrode and not to other side metabolic reactions inside the bacteria. Moreover, this approach combines advantages from both prevailing biofuel cell systems; on the one hand, enzyme-based systems that afford high enzymatic load and specific reactions that do not allow side reactions. On the other hand, microbial fuel cells, in which microorganisms can regenerate enzymatic catalysts as needed, however allow loss of electrons to other reactions in the microorganism’s metabolism. By surface displaying and attaching the redox enzymes to the electrode, we were able to combine the advantages suggested by both systems, thus overcoming the hurdles encountered when using only one of the systems.

As a first step we set out to confirm the activity and surface display of our three mutants and the incorporation of the UAA. We measured ~85% of wild-type (WT) enzyme activity for each of the three mutants with incorporated Az-Phe (Figure S2), indicating that interference with activity was minimal upon mutation and UAA incorporation. This is in contrast to other systems for site-specific immobilization through cysteine mutations, that have shown significantly decreased enzymatic activity, possibly due to multiple mutations (i.e., cysteine deletions as well as site-specific cysteine incorporation).²⁴ However, by demonstrating retention of biochemical activity, we show that ADHII was indeed expressed in *E. coli*. In order to further prove its location on the surface of the microorganism, as opposed to localization in the cytoplasm, we attempted to link the enzyme both to gold nanoparticles and to a gold surface. Figure 2 shows atomic force microscopy (AFM) and transmission electron microscopy (TEM) images of the site-specific attachment of bacteria to a gold-coated surface (Figure 2a,b) or to gold nanoparticles (Figure 2d).

The mutant shown in these images is V66TAG (results are similar with all three mutants). The images in Figure 2a,b,d could be seen only when all components of the designed system were present: bacteria harboring a plasmid encoding for the UAA incorporation (pSup-MjAzRS-6TRN),²⁵ a plasmid encoding for the autodisplay of ADHII (pJM7-ADHII), growth in the presence of Az-Phe and ‘clicking’ to **2**. When any of these components was missing, for example, in the absence of pSup-

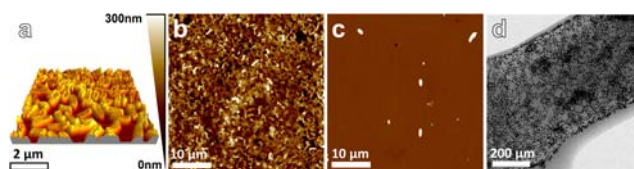


Figure 2. *E. coli* following “click” reaction with linker **2**. (a–c) AFM images. (a) 3D image of *E. coli* (V66TAG ADHII) covalently attached to gold; (b) wider field image of V66TAG ADHII; (c) *E. coli* harboring only pJM7-ADHII. (d) TEM image of Au nanoparticles covalently attached to *E. coli* V66TAG ADHII.

MjAzRS-6TRN (Figure 2c), in the absence of Az-Phe or in the absence of pJM7-ADHII, negligible numbers of bacteria on gold or gold nanoparticles on bacteria were observed.

These results indicate that only with the encoded components inserted into the system, the ‘click’ reaction occurs, affording bacteria attachment to gold, which implies the site-specific attachment of ADHII to the surface. After attachment of bacteria, we aimed to regenerate the gold surface by electrochemical reduction of the thiols at the gold surface, resulting in their detachment. The potential of the gold-coated slide was biased to -1.0 V vs Ag/AgCl reference electrode for 5 min. From an AFM image of the surface after application of potential, it could be seen that most bacteria were detached from the surface after application of potential (Figure S3). Solutions containing bacteria after desorption that were concentrated and spread onto agar plates showed growth of colonies, indicating that the bacteria remained alive after electrolysis, demonstrating that bacteria were alive before the application of potential. In addition, we investigated whether the ‘click’ reaction conditions are biocompatible, through counting viable colonies (SI section); we detected a considerable difference in the numbers of live cells upon the switch between a nonbiocompatible ligand (**4**) in the SI to the biocompatible one (**5**), (Figure S4), from 5×10^8 to 6×10^9 cells per mL, respectively, compared to control cells that did not undergo the ‘click’ reaction under the same conditions that had reached 8×10^9 cells per mL.

To assess the distribution of thiol groups and through them the distribution of the surface displayed enzymes, we attempted to attach gold nanoparticles to the modified bacteria, followed by visualization of the bacteria by TEM. Figure 2d shows the results of the TEM imaging, demonstrating that the distribution of gold nanoparticles is fairly even. According to a rough analysis of the numbers of nanoparticles per bacterium (NPB), we estimate $\sim 10\,000$ (± 1700) NPB. Due to the size of nanoparticles, we estimate that, on average, only one enzyme was attached to each particle. Based on displayed ADHII activity measurements, we estimated $\sim 11\,000$ active enzyme copies per *E. coli* cell (Figure S2). A number that corresponds well with the TEM images estimations based on the attachment of NPB.

Next, we set out to prove that the ‘click’ reaction was indeed specific; that it did take place on the surface of the bacteria on the ADHII. We ‘clicked’ the surface displayed ADHII with incorporated Az-Phe to the fluorescent probe **3**, which is an alkyne-modified rhodamine. The observation of a red fluorescent band on an SDS-PAGE gel of a size that corresponds to the ADHII monomer (33 kDa) and the absence of any other fluorescent bands demonstrate that the Az-Phe amino acid is indeed incorporated to ADHII and that the enzyme is on the surface of the bacteria, since after

performing the “click” reaction on a whole bacteria, we separated membranes from cytosolic components. Figure S5 shows fluorescent gels of the three mutants that were expressed in the presence and absence of Az-Phe. No bands were observed in the absence of the UAA. To prove that the UAA was incorporated in the intended location in ADHII and that no other natural amino acid was incorporated instead, an MS/MS analysis of a peptide that contained the UAA was performed following trypsin digest of a mutant P182TAG enzyme (Figure S6). Indeed, we could observe a peptide containing Az-Phe in position 182 instead of proline.

Next, we tested whether the displayed enzyme was able to communicate with the electrode via the site specifically linked redox linker. Hence, we attached the modified bacteria to screen printed gold electrodes and analyzed the cyclic voltammograms of the modified bacteria in the presence or absence of 1% ethanol (the natural substrate of ADHII). Upon oxidation of ethanol we expected to observe the evolution of an anodic bioelectrocatalytic current resulting from the enzymatic oxidation of ethanol, whereas in the absence of ethanol, only the typical redox wave of the redox label (2) should be observed. Figure 3 displays the evolved bioelectrocatalytic

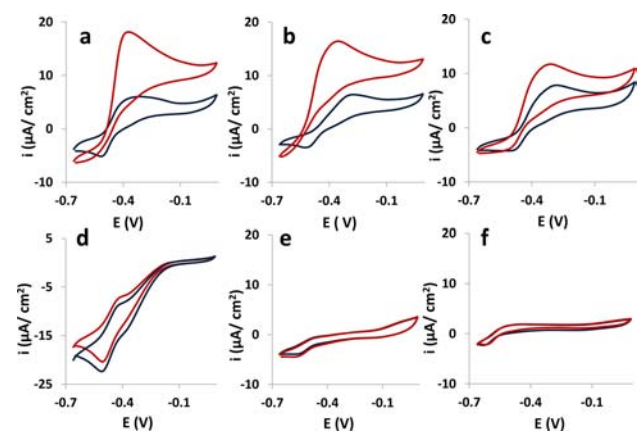


Figure 3. Cyclic voltammograms of *E. coli* attached to gold working electrode, upon a click reaction with 2. Red curves are recorded after addition of 1% ethanol. *E. coli* (a) V66TAG ADHII, (b) P182TAG ADHII, (c) D314TAG ADHII, (d) harboring pJM7-ADHII, nonspecifically attached to electrode, (e) harboring only pJM7-ADHII in solution, (f) V66TAG ADHII grown in the absence of Az-Phe. Reference electrode: pseudo Ag/AgCl; scan rate: 5 mV/s.

current in the presence of mutants V66TAG and P182TAG (Figure 3a,b, respectively), while with mutant D314TAG (c) or with a surface displayed WT ADHII, which was nonspecifically attached to the electrode (d), this current was nearly absent, indicating that both the orientation of the enzyme relative to the electrode and the distance of the redox active linker from the enzyme active site are crucial for effective active site–electrode communication. As expected, bacteria that were harboring only pJM7-ADHII or harboring both plasmids but grown in the absence of the UAA did not display any bioelectrocatalytic signals (Figure 3e,f, respectively).

Finally, we assembled a biofuel cell based on the site-specific attachment scheme as an anode. The cathode was controlled by a potentiostat^{26,27} and was biased continuously at +700 mV vs Ag/AgCl electrode. The fuel at the anode was ethanol, and the fuel cell was not compartmentalized with a membrane and was exposed to the ambient atmosphere.

The performance of the biofuel cell is shown in Figure 4. Figure 4A shows the power outputs for the mutants and their

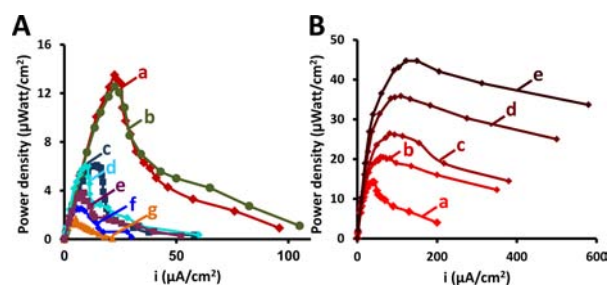


Figure 4. (A) Power densities of fuel cells constructed with *E. coli* attached to gold-coated plates, following “click” reaction with 2. *E. coli* (a) V66TAG, (b) P182TAG, (c) D314TAG, and (d) harboring pJM7-ADHII, nonspecifically attached to electrode. (e) Purified ADHII, nonspecifically attached to electrode. (f) *E. coli* harboring pJM7-ADHII, in solution. (g) WT *E. coli* in solution. (B) Power densities of a fuel cell constructed with wired *E. coli* V66TAG over a week of operation. After days: (a) 1; (b) 2; (c) 4; (d) 6; and (e) 7. Measurements were performed under ambient temperature, in the presence of 2% ethanol. A potential of +700 mV vs Ag/AgCl was applied to the cathode to simplify biofuel cell construction.

controls, where as Figure 4B shows the power outputs achieved in the system upon an operation of a week under the same conditions. Maximal performance was achieved for mutants V66TAG and P182TAG, 13.5 and 12.6 $\mu\text{W}/\text{cm}^2$ by assembling a biofuel cell and modifying the external resistances serially (Figure 4A, curves a,b, respectively). Mutant D314TAG as well as the nonspecifically bound surface displayed WT ADHII have shown similar power outputs of ~ 6.1 and $6.0 \mu\text{W}/\text{cm}^2$ (curves c,d), respectively. Purified ADHII from *Saccharomyces cerevisiae*, nonspecifically covalently bound, shows a lower power output of $3.8 \mu\text{W}/\text{cm}^2$ (curve e). ADHII concentration was similar to the estimated active enzyme units as the surface displayed ADHII (Figure S2). Surface displayed ADHII and WT *E. coli* in solution have shown minimal power outputs of 2.60 and 1.68 $\mu\text{W}/\text{cm}^2$ (curves g,f), respectively. The results achieved for mutants V66TAG and P182TAG show comparable power outputs to electrogenic bacteria in biofuel cells. When the fuel cell was operated for the duration of a week (in the presence of required antibiotics, to select against nonspecific bacteria), biofilm formation was observed in addition to a day-to-day increase in power densities. Power densities grow, and we suggest that its increase is caused by the increase in bacterial population density and concomitant (and accelerated) production and secretion of redox active molecules. These new bacteria are not covalently attached, however, without the first layer of modified bacteria, *E. coli* produce extremely low power densities. Figure 4B demonstrates the increase in power outputs over time, where maximal power outputs measured were ~ 14 , 21, 26, 36, and 45 $\mu\text{W}/\text{cm}^2$ shown in curves a–e, respectively. When an attempt was made to do the same experiment with bacteria that were displaying ADHII and were bound in a nonspecific manner to the electrode, a test of cell viability showed that the cells died (only 1% survived).

In summary, we demonstrate that the UAA Az-Phe was successfully incorporated into a surface displayed enzyme in a site-specific manner. Bacteria containing the incorporated UAA were specifically attached to gold and electrochemically desorbed from the gold surface. Excitingly, bacteria with the appropriate mutation showed bioelectrocatalytic activity and

were still viable after immobilization to the surface. Moreover, a biofuel cell was assembled with modified bacteria as the anode and has shown increasing power output performance for a week, at comparable power outputs reported in many previously reported microbial fuel cells.²⁸ In addition, no membrane was needed, and it could operate under ambient aerobic conditions. Comparing the performance of the biofuel cells to a purified enzyme or nonspecifically bound displayed enzymes has shown a superior performance for our system, which demonstrates the advantages of this approach. Currently we are investigating the source of this exciting behavior as well as the electron-transfer characteristics between the modified bacteria and electrodes. It is our belief that we were able to devise a plausible first site-specific route to achieve an important step in the direction of a true hybrid between a living microorganism and an inorganic electrode.

■ ASSOCIATED CONTENT

📄 Supporting Information

Full experimental details. This material is available free of charge via the Internet at <http://pubs.acs.org>.

■ AUTHOR INFORMATION

Corresponding Author

meijler@bgu.ac.il; alfontal@exchange.bgu.ac.il

Notes

The authors declare no competing financial interest.

■ ACKNOWLEDGMENTS

Research was supported by an Israel Science Foundation (ISF) F.I.R.S.T. Program (763/07, L. Alfonta) and by an ISF Converging Technologies Program (1693/07, L.A. and M.M.M.). Some research leading to these results received funding from the European Research Council ERC grant agreement no. 260647 (L.A.) as well as the Safra Center for the study and engineering of functional biopolymers at BGU (L.A. and M.M.M.). L.A. is the incumbent of the Elaine S. and Alvin W. Wene Career Development Chair in Biotechnology Engineering. L. Amir acknowledges a Converging Technologies and a Kreitman school for graduate students Negev fellowships. We gratefully acknowledge Prof. Peter G. Schultz for providing the pSup-MjAzRS-6TRN plasmid, Prof. Thomas Meyer for generously providing *E. coli* JK321 strain and pJM7 plasmid, and Prof. Yuval Shoham for the *Z. mobilis* genome. TEM operation by Dr. Yael Kalisman provided an invaluable contribution. We also thank: Dr. Yohai Dayagi, Sviatlana Smolskaya, Nadav Konyo, Aya Naveh, Roxana Golan, and Jürgen Jopp for technical assistance.

■ REFERENCES

- (1) Bardea, A.; Katz, E.; Bückmann, A. F.; Willner, I. *J. Am. Chem. Soc.* **1997**, *119*, 9114.
- (2) Antiochia, R.; Gorton, L. *Biosens. Bioelectron.* **2007**, *22*, 2611.
- (3) Wang, J. *Electroanalysis* **2004**, *17*, 7.
- (4) Arenkov, P.; Kukhtin, A.; Gemmell, A.; Voloshchuk, S.; Chupueva, V.; Mirzabekov, A. *Anal. Biochem.* **2000**, *278*, 123.
- (5) Katz, E.; Privman, V. *Chem. Soc. Rev.* **2010**, *39*, 1835.
- (6) Amir, L.; Tam, T. K.; Pita, M.; Meijler, M. M.; Alfonta, L.; Katz, E. *J. Am. Chem. Soc.* **2008**, *131*, 826.
- (7) Minteer, S. D.; Liaw, B. Y.; Cooney, M. J. *Curr. Opin. Biotechnol.* **2007**, *18*, 228.
- (8) Willner, I.; Katz, E. *Angew. Chem. Intl. Ed.* **2000**, *39*, 1180.

- (9) Rowe, C. A.; Leonard, M.; Feldstein, M. J.; Golden, J. P.; Scruggs, S. B.; MacCraith, B. D.; John, J.; Ligler, F. S. *Anal. Chem.* **1999**, *71*, 3846.
- (10) Besteman, K.; Lee, J. O.; Wiertz, F. G. M.; Heering, H. A.; Dekker, C. *Nano Lett.* **2003**, *3*, 727.
- (11) Riklin, A.; Katz, E.; Wiliner, I.; Stocker, A.; Bückmann, A. F. *Nature* **1995**, *376*, 672.
- (12) Ferapontova, E.; Schmengler, K.; Borchers, T.; Ruzgas, T.; Gorton, L. *Biosens. Bioelectron.* **2002**, *17*, 953.
- (13) Mrksich, M.; Whitesides, G. M. *Trends Biotechnol.* **1995**, *13*, 228.
- (14) Mrksich, M. *Chem. Soc. Rev.* **2000**, *29*, 267.
- (15) Coman, V.; Gustavsson, T.; Finkelstein, A.; von Wachenfeldt, C.; Hägerhäll, C.; Gorton, L. *J. Am. Chem. Soc.* **2009**, *131*, 16171.
- (16) Maurer, J.; Jose, J.; Meyer, T. F. *J. Bacteriol.* **1997**, *179*, 794.
- (17) Chin, J. W.; Santoro, S. W.; Martin, A. B.; King, D. S.; Wang, L.; Schultz, P. G. *J. Am. Chem. Soc.* **2002**, *124*, 9026.
- (18) Kolb, H. C.; Finn, M. G.; Sharpless, K. B. *Angew. Chem., Int. Ed.* **2001**, *40*, 2004.
- (19) Georgiou, G.; Stephens, D. L.; Stathopoulos, C.; Poetschke, H. L.; Mendenhall, J.; Earhart, C. F. *Protein Eng.* **1996**, *9*, 239.
- (20) Boder, E. T.; Wittrup, K. D. *Nat. Biotechnol.* **1997**, *15*, 553.
- (21) Fishilevich, S.; Amir, L.; Fridman, Y.; Aharoni, A.; Alfonta, L. *J. Am. Chem. Soc.* **2009**, *131*, 12052.
- (22) Szczupak, A.; Kalman, D. K.; Alfonta, L. *Chem. Commun.* **2012**, *48*, 49.
- (23) Katz, E.; Willner, I. *J. Am. Chem. Soc.* **2003**, *125*, 6803.
- (24) Holland, J. T.; Lau, C.; Brozik, S.; Atanassov, P.; Banta, S. *J. Am. Chem. Soc.* **2011**, *133*, 19262.
- (25) Ryu, Y.; Schultz, P. G. *Nat. Methods* **2006**, *3*, 263.
- (26) Schröder, U.; Nießen, J.; Scholz, F. *Angew. Chem. Intl. Ed.* **2003**, *42*, 2880.
- (27) Bond, D. R.; Lovley, D. R. *Appl. Environ. Microbiol.* **2003**, *69*, 1548.
- (28) Rabaey, K.; Verstraete, W. *Trends Biotechnol.* **2005**, *23*, 291.